analytical chemistry

pubs.acs.org/ac Article

# Resolving Ultraviolet–Visible Spectra for Complex Dissolved Mixtures of Multitudinous Organic Matters in Aerosols

Nan Xu, Min Hu,* Xiao Li, Kai Song, Yanting Qiu, Hao Xuan Sun, Yujue Wang, Linghan Zeng, Mengren Li, Hui Wang, Shuya Hu, Taomou Zong, Yao Bai, Zhou Zhang, Shuangde Li, Shijin Shuai, Yunfa Chen, and Song Guo

Cite This: *Anal. Chem.* 2024, 96, 1834–1842 Read Online

ACCESS | Metrics & More | Article Recommendations | Supporting Information

**ABSTRACT:** Light-absorbing organic aerosols, referred to as brown carbon (BrC), play a vital role in the global climate and air quality. Due to the complexity of BrC chromophores, the identified absorbing substances in the ambient atmosphere are very limited. However, without comprehensive knowledge of the complex absorbing compounds in BrC, our understanding of its sources, formation, and evolution mechanisms remains superficial, leading to great uncertainty in climatic and atmospheric models. To address this gap, we developed a constrained non-negative matrix factorization (NMF) model to resolve the individual ultraviolet–visible spectrum for each substance in dissolved organic aerosols, with the power of ultrahigh-performance liquid chromatography-diode array detector-ultrahigh-resolution mass spectrometry (UHPLC-DAD-UHRMS). The resolved spectra were validated by selected standard substances and validation samples. Approximately 40,000 light-absorbing substances were recognized at the MS1 level. It turns out that BrC is composed of a vast number of substances rather than a few prominent chromophores in the urban atmosphere. Previous understanding of the absorbing feature of BrC based on a few identified compounds could be biased. Weak-absorbing substances missed previously play an important role in BrC absorption when they are integrated due to their overwhelming number. This model brings the property exploration of complex dissolved organic mixtures to a molecular level, laying a foundation for identifying potentially significant compositions and obtaining a comprehensive chemical picture.

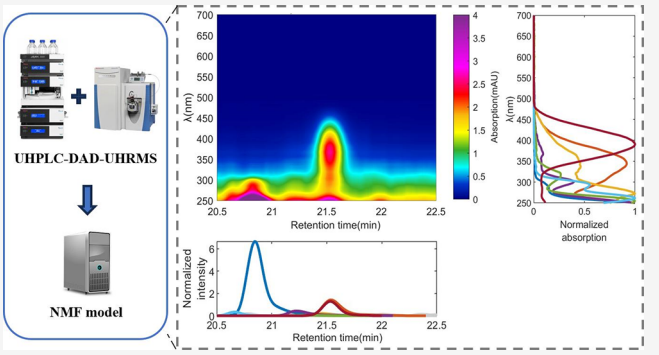




Aerosols are the carbon sinks of natural and anthropogenic organic matter in the atmosphere, playing a vital role in the global carbon cycle. Multitudinous organic compounds with a wide variety of properties contribute up to 90% mass of aerosols.[1] The organic aerosols absorbing light in near-UV and visual ranges in the atmosphere are referred to as brown carbon (BrC).[2] Its absorbing capacity directly contributes to the radiative forcing, leading to global warming and visibility reduction. The interaction with radiation can also influence atmospheric photochemical reactions, making an impact on air quality.[3]

However, our understanding of the absorption characteristics and climate impacts of BrC remains highly incomplete and uncertain.[4,5] The estimated direct radiative effect of BrC absorption ranges widely from +0.03 to +0.6 W/m$^2$ in different climate models.[6−9] The diversity of chemical compositions from various sources leads to huge distinctions in the absorption properties. Therefore, the inadequate emission inventories and inconsistent absorbing parameters used in different models may cause great deviation.[4] The establishment of the intrinsic relationship between the chemical composition and light absorption at the molecular level is the key to clarifying the absorption characteristics of various sources and evolution processes of BrC in the atmosphere, which lays a foundation for accurate model representations.[10]

Therefore, researchers have been working on discovering light-absorbing substances, but the identified chromophores in the ambient atmosphere are still very limited,[10] only accounting for less than 10% in the urban atmosphere.[11] Besides, the top BrC molecules proposed by different identification methods for the same type of aerosols were significantly distinct.[12,13] Without comprehensive knowledge, we have no idea about how well these identified compounds can represent the bulk property. Previously, it was believed impossible to identify all molecules responsible for light

**Received:** June 20, 2023
**Revised:** December 26, 2023
**Accepted:** January 3, 2024
**Published:** January 24, 2024

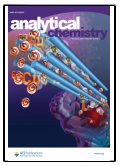





https://doi.org/10.1021/acs.analchem.3c02700
*Anal. Chem.* 2024, 96, 1834–1842

absorption, much less to obtain the individual spectrum for each compound in aerosols, due to the complexity of BrC chromophores.[14] However, with the development of instrument technology and computing science, the idea of apportioning the absorption spectrum to entire molecules in aerosols could be realized. Methanol is able to extract nearly 90% of BrC,[10] turning organic aerosols into dissolved mixtures. The appearance of a hyphenated technique named ultrahigh-performance liquid chromatography-diode array detector-ultrahigh-resolution mass spectrometry (UHPLC-DAD-UHRMS) brings the absorption measurement of complex dissolved mixtures to the molecular level. The ultraviolet−visible (UV−vis) spectra of separated eluates are constantly detected by DAD. Meanwhile, all detectable substances including abundant unknown compounds are analyzed when UHRMS works in full scan mode. However, the amount of dissolved organic substances in aerosols is too giant, leading to numerous overlapping peaks in DAD. Therefore, it is necessary to develop a deconvolution model for the resolution of overlapping spectra with the power of the computers.

Although many models have been proposed and applied to the decomposition of LC-DAD data over the years,[15−25] they can hardly be put into practical use when it comes to multitudinous organic mixtures in nature since they are designed for target analysis of several known analytes. First, most models require the number of compounds in dissolved mixtures to be known, which is almost impossible for organic aerosols. Besides, when the peaks are heavily or even completely overlapping, these models can hardly provide reliable and accurate results. Finally, it is difficult to interpret the resolution results since most substances are unknown. However, with the abundant information provided by UHRMS, these defects can be overcome.

Taking methanol-dissolved organic aerosols as an example, we developed a constrained non-negative matrix factorization (NMF) model to obtain the individual UV−vis spectrum for each substance, with the power of UHPLC-DAD-UHRMS. Especially, the MS1 peaks measured by UHRMS in full scan mode were used as the initial input parameter, so the deconvoluted DAD spectra can be directly assigned to corresponding substances. The resolved spectra are validated by selected standard substances and validation samples. In this paper, our primary focus lies in illustrating the model theory and validating the results. Additionally, we compare our model with previous studies and discuss its application prospects and limitations. The analysis of molecular characteristics for the resolved absorbing substances from various sources and ambient samples will be addressed elsewhere.

## EXPERIMENTAL SECTION

**Collection of Aerosol Samples.** A total of 54 aerosol samples were collected, consisting of 40 samples from various sources and 14 samples from the ambient atmosphere. Particulate samples from primary emissions (biomass burning, cooking, coal burning, nonroad diesel engine, gasoline engine) were collected by a homemade sampler,[26] with a flow rate of around 10 L/min. Typical secondary formation samples (aqueous reactions of methylglyoxal with ammonium sulfate, MG+AS) were also included. A detailed description of source samples can be found in Table S1. Atmospheric $PM_{2.5}$ samples were collected in June 2018 and November 2018 in Beijing by a high-volume sampler (TH-1000C, Tianhong, China) with a flow rate of 1.05 $m^3$/min. Details of ambient samples are presented in Table S2. Among them, two samples were used for validation. The remaining 52 samples were used for computing.

**Extraction of the Organic Constituent.** Most samples were collected on prebaked (550 °C for 5.5 h) quartz-fiber filters, except MG+AS, which was directly reacted in an aqueous solution. Organic matters on filters were dissolved into methanol by ultrasonic extraction to investigate absorbing molecular characteristics using UHPLC-DAD-UHRMS. First, small pieces with a total load of 300−400 μg of organic carbon (OC) were cut out from each filter. Then they were extracted using 5, 4, and 3 mL of methanol (Optima LC/MS, Thermo Fisher Scientific) sequentially in an ultrasonic bath filled with ice water for 20 min each time. The methanol extracts were filtered through polytetrafluoroethylene syringe filters (wwPTFE, 0.2 μm, Pall Corporation) and evaporated to dryness under a gentle stream of high-purity nitrogen gas. Finally, 300 μL of methanol containing 1 μg/mL internal standard (Table S3) was used to redissolve each extract before the centrifugation for 2 min at 15,000 rpm.

**Analysis of Dissolved Organic Aerosols.** The methanol extracts or aqueous reaction productions are extremely complex dissolved mixtures of organic matters. The crucial analysis work was powered by a UHPLC-DAD system (Ultimate 3000, Thermo Fisher Scientific) coupled with an Orbitrap UHRMS (Exactive Plus, Thermo Fisher Scientific). After a 2 μL injection, light-absorbing compounds were separated by an ultraperformance reverse phase column (Acquity UPLC HSS T3, 2.1 × 150 mm, 1.8 μm particle size, Waters) with a precolumn (VanGuard HSS T3, 2.1 × 5 mm, 1.8 μm particle size, Waters) at 40 °C. A gradient elution procedure was performed with a binary mobile phase composed of (A) ultrapure water (>18 MΩ cm, Milli-Q) with 0.1% (v/v) acetic acid and (B) methanol (Optima LC/MS, Thermo Fisher Scientific) at a flow rate of 0.2 mL/min. The elution protocol started from 0% B for the first 1 min, linearly increasing to 100% B in 1−70 min, and held at 100% B for the next 13 min. Then phase B rapidly dropped to 0% in 1 min and maintained 0% until the end of the procedure (90 min) so that the column could be balanced at the initial state, ready for the next injection. After separation, the UV−vis absorption spectra of the eluates were measured by the DAD detector every 1 nm over the wavelength range of 250−700 nm. DAD signals were deducted by a solvent blank for all samples to avoid the influence of gradient elution.

Eventually, these eluates were further identified and semiquantified by UHRMS based on $m/z$ values and signal intensities. Both the heated electrospray ionization (HESI) source and atmospheric pressure chemical ionization (APCI) source were applied to achieve better ionization efficiency in a wide range of polarities. The ionization source can switch quickly between the positive and negative modes, so analytes were detected in both modes simultaneously by one injection. HESI source worked at a spray voltage of ±3.5 kV and a capillary temperature of 320 °C, along with 40 units of sheath gas flow and 10 units of auxiliary gas flow. APCI source worked at the spray voltage of ±5.0 kV, with 20 units of sheath gas flow and 5 units of auxiliary gas flow. The capillary temperature was 225 °C, and the vaporizer temperature was 350 °C. Data acquisition was carried out at a mass range of $m/z$ 60−900, with a resolution of 70,000 at $m/z$ 200.

**Data Processing of UHRMS.** The UHRMS data determined by Orbitrap were initially processed using MZmine


https://doi.org/10.1021/acs.analchem.3c02700
Anal. Chem. 2024, 96, 1834−1842

2.53[27] (http://mzmine.github.io/) for mass detection, chromatogram construction and deconvolution, peak alignment, isotopic peak grouping, and formula prediction. Main parameters applied in each step are shown in Table S4. With these steps, a preliminary nontarget MS1 peak list assigned with molecular formulas in each mode (ESI+, ESI−, APCI+, and APCI−) was achieved. As most isomers were separated by UHPLC to a great extent, these peaks could represent substances other than formulas. Peaks detected in blank samples were not removed since they were also absorption contributors in DAD. MATLAB R2022a was applied for further chromatogram extractions based on the $m/z$ and retention time information in the peak list built by MZmine. Those peaks of which the retention times were rather close (within 0.2 min) and the intensities among all source and ambient samples were highly linearly correlated ($R > 0.95$) were considered as the analyte and its adducts. Only the peak with the largest intensity was retained. Many compounds were detected in multiple modes. The one with the highest intensity was kept when integrating the peak lists in different modes.

**Calculation of Optical Parameters.** The optical parameters of the standard substances and dissolved mixtures of organic aerosols in methanol were both determined by a UV−vis spectrometer (UV-1780, Shimadzu) and a DAD. With the absorption spectra measured by UV−vis spectroscopy, the bulk mass absorption coefficient ($MAC_{bulk}$) of aerosol organic mixtures or the MAC of standard substances was calculated as[10]

$$\mathrm{MAC}\ (\mathrm{m^2\ g^{-1}}) = \frac{A_{uvs} \times \ln(10)}{l\ (\mathrm{m}) \times C_{sol}\ (\mathrm{ng\ \mu L^{-1}})} \quad (1)$$

where $A_{uvs}$ is the base-10 absorbance at each wavelength acquired by the UV−vis spectroscopy, l is the path length of the cuvette (0.01 m), and $C_{sol}$ is the corresponding mass concentration of organic matters in the solution. For aerosol samples, $C_{sol}$ cannot be measured directly in an organic solvent. Since methanol is considered to extract most organic matters,[28,29] the OC measured by an OCEC analyzer (Sunset Laboratory) was used to calculate $C_{sol}$. The corresponding MAC values calculated should be considered as a lower limit.

To present the absorption contribution of the light-absorbing compounds in an ambient atmosphere, the bulk absorption coefficient ($b_{abs\text{-}bulk}$) was calculated as follows:[10]

$$b_{abs-bulk}\ (\mathrm{Mm^{-1}}) = \mathrm{MAC}_{bulk}\ (\mathrm{m^2\ g^{-1}}) \times C_{air}\ (\mathrm{\mu g\ m^{-3}}) = \frac{A_{uvs} \times \ln(10) \times V_{sol}\ (\mathrm{mL}) \times S\ (\mathrm{cm^2})}{l\ (\mathrm{m}) \times V_{air}\ (\mathrm{m^3}) \times S_{ext}\ (\mathrm{cm^2})} \quad (2)$$

where $C_{air}$ is the mass concentration of organic aerosols in the atmosphere. $V_{air}$ is the sampling volume, $V_{sol}$ is the volume of the extracting solvent, $S$ is the entire sampling filter area, and $S_{ext}$ is the extracted filter area.

Molecular absorption spectra of each compound can be obtained in the decomposed DAD matrix. Then the molecular MAC ($MAC_{mole}$) was calculated as[30,31]

$$\mathrm{MAC}_{mole}\ (m^2 g^{-1}) = \frac{A_{DAD}\ (\mathrm{mAU\ min}) \times F\ (\mathrm{mL\ min^{-1}}) \times \ln(10)}{l\ (\mathrm{m}) \times C_{sol}\ (\mathrm{ng\ \mu L^{-1}}) \times V_{inj}\ (\mu\mathrm{L})} \quad (3)$$

where $A_{DAD}$ is the integrated peak area of the corresponding $\widehat{X}_i$ at any wavelength resolved by our model (Supporting Information), $F$ is the LC flow rate, $l$ is the path length of the DAD optical cell (0.007 m), and $C_{sol}$ is the mass concentration of the specific compound in the injection, and $V_{inj}$ is the injection volume. The formula can also be used to calculate the $MAC_{bulk}$ of mixtures when $A_{DAD}$ is the total area of the DAD chromatogram at any wavelength and $C_{sol}$ refers to the total mass concentration of the organic mixtures in methanol.

Unfortunately, the exact mass concentrations of most organic matter are unknown unless their standards are available. However, the equivalent mass concentrations can be achieved by their relative MS1 intensities and the concentrations of the internal standards. Therefore, the molecular equivalent mass absorption coefficient (EMAC) was proposed:

$$\mathrm{EMAC}\ (\mathrm{m^2\ g^{-1}}) = \frac{A_{DAD}(\mathrm{mAU\ min}) \times F(\mathrm{mL\ min^{-1}}) \times \ln(10) \times I_{IS} \times \mathrm{MW}_{IS}}{l\ (\mathrm{m}) \times I_{mole} \times \mathrm{MW}_{mole} \times C_{IS}\ (\mathrm{ng\ \mu L^{-1}}) \times V_{inj}\ (\mu\mathrm{L})} \quad (4)$$

where $I_{mole}$ and $\mathrm{MW}_{mole}$ are the integral area of the extracted ion peak at MS1 and the molecular weight of the compound, respectively, while $I_{IS}$ and $\mathrm{MW}_{IS}$ refer to those of the internal standard. $C_{IS}$ represents the mass concentration of the internal standard. With EMAC, the molecular absorption coefficient ($b_{abs\text{-}mole}$) can be calculated as

$$\mathrm{b}_{abs-mole}\ (\mathrm{Mm^{-1}}) = [\mathrm{EMAC}\ (\mathrm{m^2\ g^{-1}}) \times I_{mole} \times \mathrm{MW}_{mole} \times C_{IS}\ (\mathrm{ng\ \mu L^{-1}}) \times V_{sol}\ (\mathrm{mL}) \times S\ (\mathrm{cm^2})]/[I_{IS} \times \mathrm{MW}_{IS} \times V_{air}\ (\mathrm{m^3}) \times S_{ext}\ (\mathrm{cm^2})] \quad (5)$$

$b_{abs\text{-}mole}$ of a known compound in new samples can be achieved just by the corresponding $I_{mole}$ and $I_{IS}$ measured by MS, instead of running the NMF model time after time. Also, the DAD chromatogram ($X$) can be roughly reconstructed by the MS data matrix of extracted ion peak ($P_0$) when EMAC for each compound is known.

**Model Development.** *Overview.* LC-DAD presents absorption of the eluates in both the wavelength and retention time domain. The acquired data are matrixes with n rows and m columns, where m refers to retention time points and n is wavelength points. The data matrix ($X$) can be decomposed into a spectrographic ($S$) matrix factor and an eluting peak ($P$) matrix factor:

$$X_{n\times m} = S_{n\times r} \times P_{r\times m} \quad (6)$$

where $r$ corresponds to the number of absorbing substances. Each column of $S$ represents the absorption spectrum of a certain substance, while each row of $P$ represents its eluting peak. Since all the elements in the $X$, $P$, and $S$ matrices are all nonnegative, the factorization is indeed a NMF problem.

52 out of 54 aerosol samples in total from various sources and the ambient atmosphere were used for computation. Since the width of an elution peak is normally less than 2 min, a moving window was applied to reduce the quantity of substances participating in each calculation, which ensures that the NMF model is solvable ($r$ should be less than the minimum of $n$ and $m$) and avoids operations and storage on a large sparse matrix. The matrix within the time window was extracted and spliced for all samples. The variance of signal intensity for each analyte in diverse samples also improved the


https://doi.org/10.1021/acs.analchem.3c02700
Anal. Chem. 2024, 96, 1834−1842

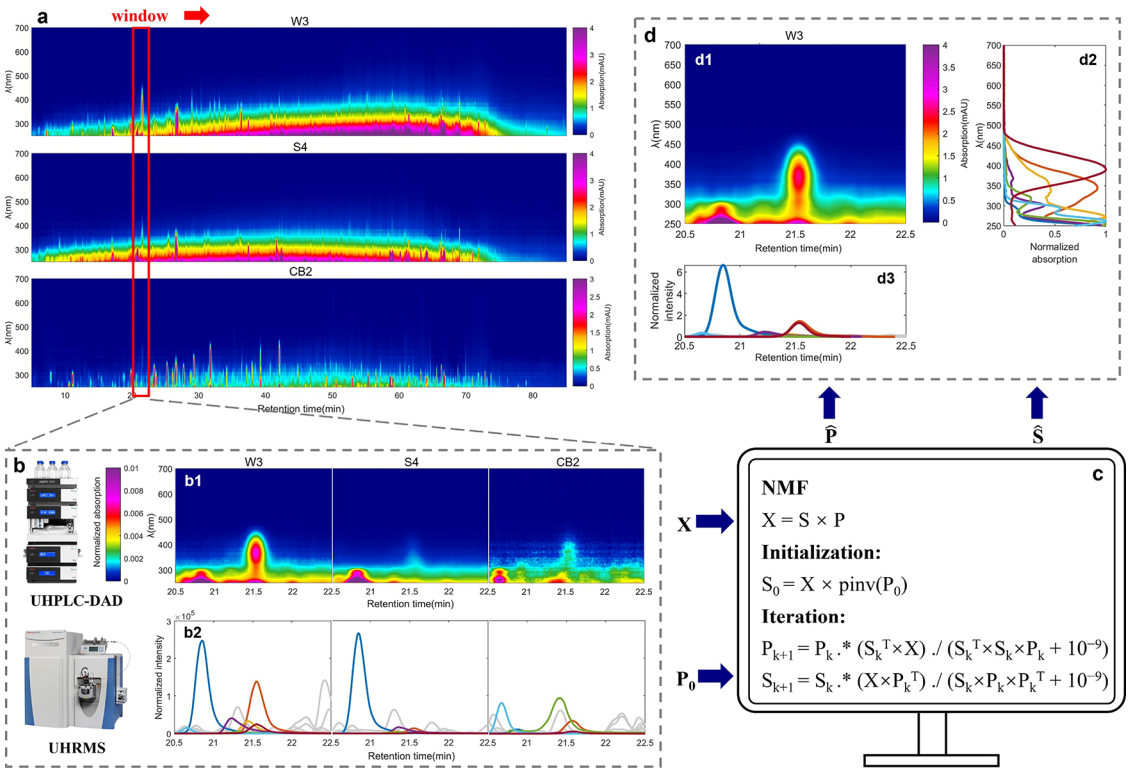


**Figure 1.** Overview of the model scheme. (a) Aligned UHPLC-DAD absorption chromatographs at various wavelengths, taking 3 of 52 samples (W3, S4, and CB2) as an example. A window of 2 min is marked. (b) Extracted and spliced data matrix by UHPLC-DAD (b1) and extracted ion peaks by UHRMS (b2) within the time window, which are normalized among samples. The colored ion peaks are for the main absorption contributors. (c) Initialization and iteration algorithm for NMF. The DAD data matrix ($X$, b1) can be decomposed into a spectrographic ($S$) matrix factor and an eluting peak matrix factor ($P$) for each molecule. The extracted peak intensity matrix (b2) directly served as the initial $P$ matrix ($P_0$). The initial $S$ matrix ($S_0$) is achieved by $X$ multiplying the Moore−Penrose pseudoinverse (pinv) of $P_0$. $T$ represents the transposition of the matrix. $k$ indicates the iteration times. With the input of $X$ and $P_0$, $\hat{P}$ and $\hat{S}$ are obtained when the iteration terminates. (d) Resolved spectra ($\hat{S}$, d2) and eluting peak ($\hat{P}$, d3) for main absorption contributors, taking W3 as an example. Colors correspond with those in b2. d1 represents the reconstructed DAD chromatogram calculated by $\hat{S} \times \hat{P}$.

model's performance. The window moved forward at a step of 0.1 min until the whole matrix was decomposed (Figure 1a,b). The model code built on MATLAB 2022a and the illustration of operation are available on GitHub (https://github.com/xnoonx/NMFDAD).

*Initialization.* The initialization condition affects the solution of the NMF problems. The closer they are to the true situation, the faster the model reaches convergence, avoiding being trapped in local optima. According to the Lambert−Beer law, the absorption contribution of an eluate at a specific wavelength should be proportional to its concentration. Since the concentration of dissolved organic matter injected into UHPLC-DAD-UHRMS was limited to a relatively low level, the ionization efficiency of an analyte was assumed to be constant. That is, the MS intensity of an eluate was also supposed to be proportional to its concentration. Therefore, the MS data matrix of the extracted ion peak based on the nontarget peak list could right serve as the initial $P$ matrix ($P_0$) (Figure 1b). The rank of factors ($r$) is equal to the number of compounds of which the retention time lies in the window according to the peak list. Each row of $P_0$ was generated by extracting and splicing the ion chromatogram within the window of a certain compound. Then the initial $S$ matrix ($S_0$) was achieved by $X$ multiplying Moore−Penrose pseudoinverse (pinv) of $P_0$ (Figure 1c). Negative elements in $S_0$ would be replaced with a tiny positive value. However, $P_0$ can be inconsistent with $P$ due to the variation of retention time and peak shape between the DAD and MS chromatogram. Besides, the ionization efficiency of a certain analyte may have a slight variation among samples influenced by different coeluting substances. These discrepancies will be corrected by the following NMF iteration.

*Iteration.* The basic iteration followed the algorithm raised by Lee and Seung[32] (Figure 1c). However, constraints need to be added according to the characteristics of the spectra and eluting peaks. First, both spectra and eluting peaks are supposed to be continuous. This was achieved by smoothing the initial $S$ matrix and $P$ matrix when initializing. Second, the eluting peak of a specific compound should be unimodal. Therefore, the $P$ matrix was constrained by cutting off the local minimums of the peak for each constituent through the iteration process. The iteration terminated when the relative change of the $S$ and $P$ matrix or the root-mean-square residual between $X$ and $S \times P$ was less than 0.01% compared to the previous iteration.

*Interpretation.* Many previous models face the problem of interpreting their decomposition results.[15−25] They can deal with only the absorption of several target substances. In our model, each row vector of the $P_0$ matrix with the corresponding column vector of the $S_0$ matrix carried the feature of a compound uniquely characterized by its molecular formula and retention time, which was maintained through


https://doi.org/10.1021/acs.analchem.3c02700
Anal. Chem. 2024, 96, 1834−1842

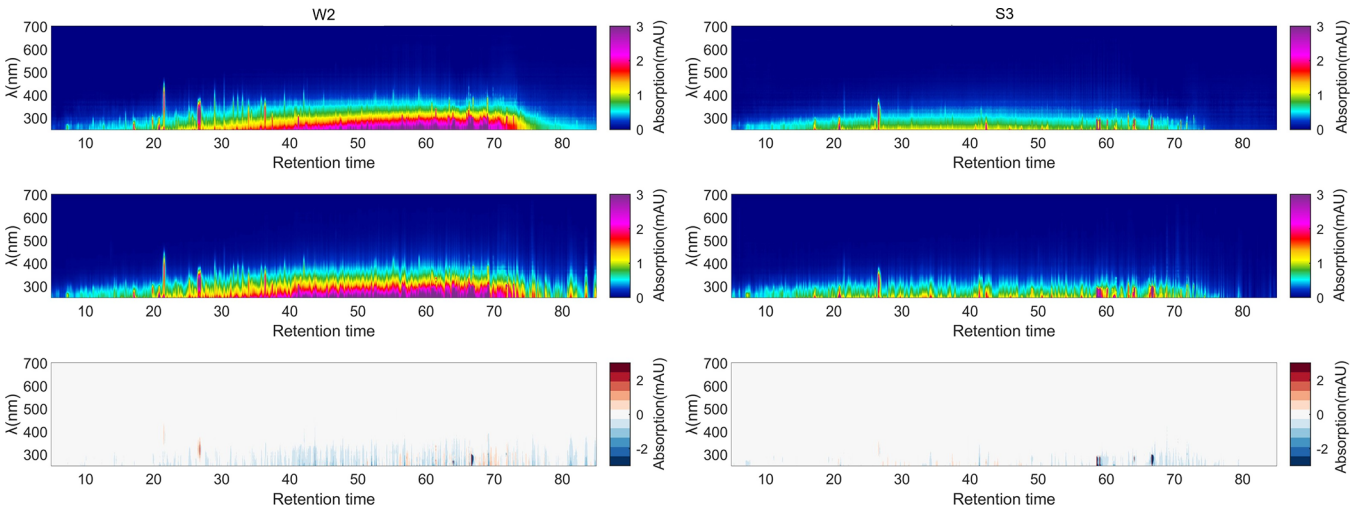


**Figure 2.** Comparison of the rebuilt and measured DAD chromatogram of the two validation samples (left for W2, right for S3). The upper two plots refer to the chromatograms measured by DAD. The middle ones are calculated by MS ion chromatograms multiplying simulated EMAC. The lower two represent the deviation of the measured and rebuilt DAD chromatogram.

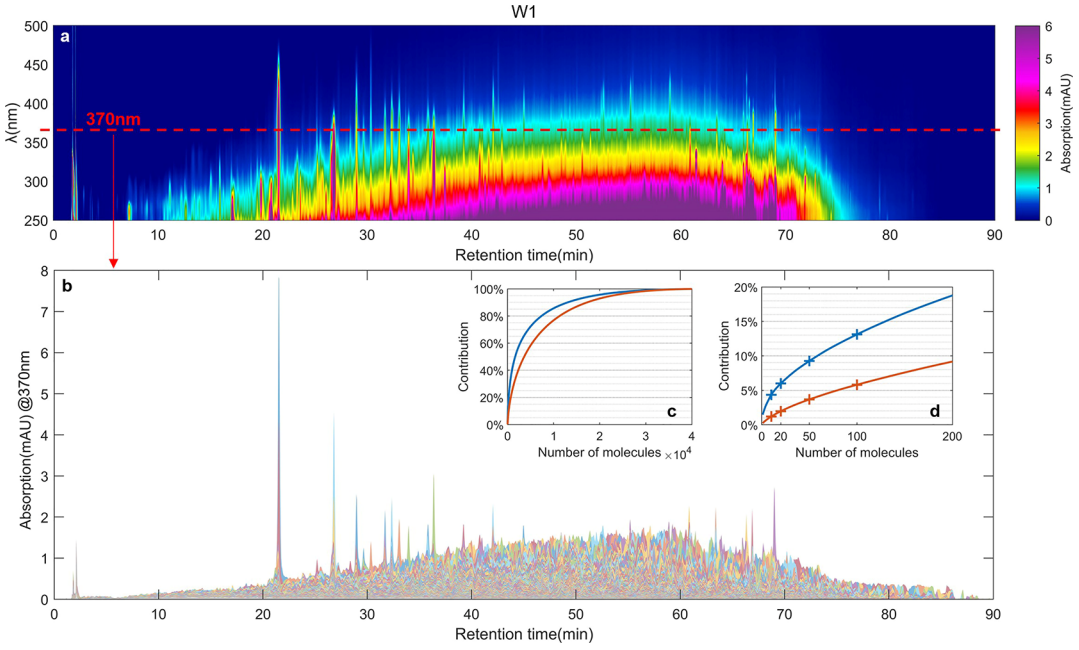


**Figure 3.** Multitudinous light absorbing substances in Beijing. (a) DAD chromatograph for sample W1 at 250−500 nm. The wavelength at 370 nm is marked. (b) Absorption chromatograph contributed by tremendous amount of substances at 370 nm. Substances are distinguished by color. (c, d) Maximum absorption contribution at 370 nm corresponding to the number of identified molecules. The blue line indicates the average value in winter Beijing, while the orange line indicates the average value in summer Beijing.

iteration. Therefore, the DAD chromatogram apportioned to a certain compound ($X_i$) can be calculated as

$$\widehat{X}_i = \widehat{S}_i \times \widehat{P}_i \tag{7}$$

in which $\widehat{S}_i$ refers to the $i$-th column in the estimated $S$ matrix, relating to the absorption spectrum of the compound. $\widehat{P}_i$ refers to the $i$-th row in the estimated $P$ matrix, relating to the eluting peak of the compound (Figure 1d). Once $\widehat{P}_i$ was recognized as a complete eluting peak in the window, $\widehat{S}_i$ and $\widehat{P}_i$ would be output to the final $\widehat{S}$ and final $\widehat{P}$ matrix. $\widehat{X}_i$ would be subtracted in the total matrix $X$, and the corresponding compound would not participate in the following calculation.

The integral peak area of $\widehat{X}_i$ was used to calculate the MAC and EMAC of the compound. The root-mean-square error (RMSE) of each sample was calculated by

$$\mathrm{RMSE} = \sqrt{\frac{1}{n \times m} \sum_{j=1}^{m} \sum_{i=1}^{n} |X_{ij} - (\widehat{S} \times \widehat{P})_{ij}|^2} \tag{8}$$

where $i$ and $j$ refer to the row and column index of the matrices. $n$ and $m$ are the row and column number. $X$ represents the measured DAD matrix of the sample, while $\widehat{S}$ and $\widehat{P}$ refer to the final $S$ and corresponding final $P$ of the sample obtained by the model. The relative RMSE (RE) was


https://doi.org/10.1021/acs.analchem.3c02700
Anal. Chem. 2024, 96, 1834−1842

defined as RMSE normalized by the root-mean-square (RMS) of $X$:

$$\mathrm{RE} = \frac{\sqrt{\frac{1}{n\times m}\sum_{j=1}^{m}\sum_{i=1}^{n}|X_{ij} - (\hat{S}\times\hat{P})_{ij}|^2}}{\sqrt{\frac{1}{n\times m}\sum_{j=1}^{m}\sum_{i=1}^{n}|X_{ij}|^2}} \times 100\% \quad (9)$$

The average RMSE among the 52 samples participating in calculation is 0.11 ± 0.08, while the average RE is 16 ± 12%.

## RESULTS AND DISCUSSION

**Evaluation of the Resolved Spectra.** To ensure the reliability of the resolved spectra, two evaluation methods were employed. First, a set of 24 substances found in aerosols, most of which are typical absorption contributors, were selected as validation compounds (Table S5). The maximum concentrations of these substances in methanol extracts among all samples vary from 0.004 to 15.6 $\mu$g mL$^{-1}$. Their standard solutions in methanol (5 $\mu$g mL$^{-1}$) were measured by UV−vis spectroscopy. The comparison of simulated and measured spectra normalized as MAC is presented in Figure S1. The correlation coefficients for all selected compounds exceed 0.9, without exception. The magnitudes of the simulated and measured spectra also matched well.

Second, two ambient samples that were not included in the computation were used for validation. The selected samples were collected in a medium polluted atmosphere in the summer and winter in Beijing, which are representative for different environments and supposed to contain most compounds from various sources. The DAD chromatogram of the validation samples was reconstructed using the MS ion peaks and EMAC obtained by our model. As the peaks in the MS chromatogram are often wider than those in the DAD chromatogram due to dispersion in elution, the reconstructed DAD chromatogram appears slightly rougher than the measured one. However, the integrated areas are comparable (Figure 2). The RMSE (RE) values between the measured DAD matrix and reconstructed matrix (smoothed by moving averages for 0.5 min) of the two validation samples are 0.07 (23%) and 0.14 (24%) in summer and winter, respectively.

**Diversity of Light-Absorbing Substances.** BrC is composed of extremely numerous organic compounds (Figure 3a,b). In winter Beijing, for example, over 80,000 substances have been detected by MZmine based on UPLC-UHRMS data, composed of approximately 10,000 formulas with abundant isomers. According to our model, around half of the substances contribute to light absorption at 370 nm. Previously, it was believed that the bulk absorption of BrC is mainly contributed by some significant chromophores.[10] However, this is not the case with ambient aerosols. The distribution of molecular absorption indicates that even the most absorbing compositions can only make a limited contribution (Figure 3c). In Beijing, for instance, the 100 most absorbing substances only contribute 13% of the total light absorption at 370 nm in winter and even less than 6% in summer (Figure 3d). This explains why the identified absorbing compounds to date only account for a very limited part in ambient aerosols, although they tend to have a strong absorb efficiency individually. Due to the overwhelming amount, weak-absorbing substances can be great contributors to BrC absorption when they are integrated.

It is necessary to investigate the heterogeneity of the absorbing properties among the numerous molecules in BrC. This also answers the question of whether minor identified compounds can explain the bulk property. According to the resolved spectra, the absorbing efficiency and wavelength dependence of each molecule show a great discrepancy. The equivalent mass absorption coefficient (EMAC) spreads over 5 orders of magnitude. The spectrum shape also varies among different molecules, typically characterized by absorption maxima. Molecules with a stronger conjugate structure usually have a larger absorption wavelength. Most of the absorption substances identified previously usually exhibit an absorption peak above 300 nm,[11] as is the case with the 10 most absorbing substances at 370 nm identified by this study (Figure S2c). However, the feature is inconsistent with the bulk spectrum shape of ambient aerosols, which monotonically decreases above 300 nm without peaks (Figure S2a). Numerous weak-absorbing substances missed previously were found to fill the knowledge gap. For many light-absorbing compounds, the maximum absorption wavelength is less than 300 or even 250 nm due to the lack of conjugation (Figure S2b). They turn out to be the largest contributor to absorption above 300 nm. In Beijing, 71% of the light-absorbing substances with no obvious absorption peak above 300 nm contribute 74% of the absorption at 370 nm on average. These compounds with a large absorption at the ultraviolet band may play a vital role in photochemical reactions, but many of them have not been paid attention to in previous studies. The diversity of light-absorbing substances in Beijing indicates that a comprehensive understanding of BrC should be achieved in a nontarget way. Previous understanding of the absorbing feature of BrC based on minor identified compounds could be biased.

**Comparison with Previous Studies.** In previous studies, two methods were commonly applied to identify light-absorbing molecules in aerosols. First, with UHPLC-DAD-UHRMS, the molecular formulas could be assigned to significant absorbing substances by comparing the retention time and intensity of the peaks between MS and DAD chromatogram manually.[11,13,30,33−49] Dozens of strong light-absorbing compounds that exhibit an obvious peak in the chromatogram have been identified by this method. The compounds and their spectra are consistent with our results. However, only a limited part of the BrC absorption could be explained due to the small number of these recognizable substances. Sometimes, the contribution of the coeluted analytes could be attributed to the identified substances, leading to an overestimation of their absorption ability. In this study, the spectra of numerous coeluted compounds are resolved by machine learning. The identification rate was increased from approximately 10% to nearly 100%. Huge amounts of weakly absorbing substances have been recognized, filling the knowledge gap of BrC chromophores to a large extent.

In the second method, the bulk absorption measured by UV−vis spectroscopy was assigned to each formula using partial least-squares regression[12,50] or random forest regression.[51] In some studies, dissolved samples were directly injected into MS to obtain the molecular formulas. The significant absorption contributors screened by this method are not comparable to our study or many other studies. Due to the common existence of isomers and strong matrix interferences between ions, the ion intensity is probably no longer proportional to the concentration or absorption, which is not in accordance with the model assumption. However, if the intensities of molecular compositions are acquired by other


https://doi.org/10.1021/acs.analchem.3c02700
Anal. Chem. 2024, 96, 1834−1842

quantitative methods like gas or liquid chromatography coupled with high-resolution mass spectrometry, the results become more reliable.[52]

**Applications.** Organic matters in nature are extremely complex mixtures with a wide variety of properties, ubiquitous among the pedosphere, hydrosphere, atmosphere, and biosphere. Special attention has been paid to their light-absorbing ability. Multitudinous substances with a tiny absorption can cause significant environmental and climatic effects when they are integrated.[10] The model developed in this work is applicable to the UV−vis absorption spectra resolution of all kinds of dissolved organic mixtures, such as BrC in the atmosphere, chromophoric dissolved organic matter (CDOM) in the hydrosphere, food coloring, or any other field in which organic chromophores matter. Comprehensive absorbing substances can be recognized in a nontarget way. The nature of light absorption at the molecular level can be comprehensively revealed at the MS1 level. When MS2 information is available, a better understanding of the molecular structures. Significant chromophores can be further investigated in a targeted manner. Studies for apportionment of the multidimensional signals detected by hyphenated instruments may also be inspired. For instance, DAD can be substituted by other detectors so that various properties can be associated with molecular compositions.

**Limitations.** In this study, organic compounds in aerosols were dissolved in methanol to study their light absorption properties. Therefore, the light absorption properties may have a slight discrepancy from those in the ambient atmosphere. Only methanol-extractable substances can be investigated, which account for nearly 90% in total BrC.[10] Chemical reactions may also take place during extraction, although protection from light and ice water ultrasound were employed for inhibition. The influence of the solvent effect on absorption is also inevitable. Additionally, the acidity of the eluent may play a significant role in light absorption. Limited by the separation ability of chromatography, the resolution of the inseparable analytes, such as strongly polar organic compounds eluted in the dead time, may not be reliable. Also, those compounds that cannot be ionized under all four ionization modes of mass spectrometry cannot be recognized. However, the purpose of this study is not to obtain precise spectra of each individual substance but to identify potential chromophores and achieve a comprehensive understanding of absorbance at the molecular level. Therefore, the absorption deviation of minor substances is acceptable.

## CONCLUSIONS

To obtain a comprehensive picture of BrC at the molecular level, we developed a constrained non-negative matrix factorization (NMF) model to simulate the individual UV−vis spectrum for each substance in dissolved organic aerosols, making full use of the abundant information provided by UHPLC-DAD-UHRMS. Samples from various sources and the ambient atmosphere were used for computation. The resolved spectra were validated by standard substances and validation samples. Both the magnitude and shape of the simulated and measured spectra matched well. Our method has greatly improved the identification ratio of absorbing substances in aerosols. Numerous weak-absorbing substances missed previously were found to fill the knowledge gap. Many ambiguous understandings of BrC chromophores have been updated. The potential application and limitations of the method are also discussed.

## ASSOCIATED CONTENT

### Supporting Information

The Supporting Information is available free of charge at https://pubs.acs.org/doi/10.1021/acs.analchem.3c02700.

Details for source and ambient samples, information for standard substances, parameters applied in MZmine, validation of simulated spectra, and absorption spectra contributed by diverse substances (PDF)

## AUTHOR INFORMATION


### Corresponding Author

**Min Hu** − *State Key Joint Laboratory of Environmental Simulation and Pollution Control, International Joint Laboratory for Regional Pollution Control, Ministry of Education (IJRC), College of Environmental Sciences and Engineering, Peking University, Beijing 100871, China;* orcid.org/0000-0002-5165-8369; Email: minhu@pku.edu.cn

### Authors

**Nan Xu** − *State Key Joint Laboratory of Environmental Simulation and Pollution Control, International Joint Laboratory for Regional Pollution Control, Ministry of Education (IJRC), College of Environmental Sciences and Engineering, Peking University, Beijing 100871, China;* orcid.org/0009-0000-9044-0947

**Xiao Li** − *State Key Joint Laboratory of Environmental Simulation and Pollution Control, International Joint Laboratory for Regional Pollution Control, Ministry of Education (IJRC), College of Environmental Sciences and Engineering, Peking University, Beijing 100871, China*

**Kai Song** − *State Key Joint Laboratory of Environmental Simulation and Pollution Control, International Joint Laboratory for Regional Pollution Control, Ministry of Education (IJRC), College of Environmental Sciences and Engineering, Peking University, Beijing 100871, China*

**Yanting Qiu** − *State Key Joint Laboratory of Environmental Simulation and Pollution Control, International Joint Laboratory for Regional Pollution Control, Ministry of Education (IJRC), College of Environmental Sciences and Engineering, Peking University, Beijing 100871, China;* orcid.org/0000-0003-2632-8621

**Hao Xuan Sun** − *Center for Data Science, Peking University, Beijing 100871, China*

**Yujue Wang** − *State Key Joint Laboratory of Environmental Simulation and Pollution Control, International Joint Laboratory for Regional Pollution Control, Ministry of Education (IJRC), College of Environmental Sciences and Engineering, Peking University, Beijing 100871, China;* orcid.org/0000-0003-4563-9214

**Linghan Zeng** − *State Key Joint Laboratory of Environmental Simulation and Pollution Control, International Joint Laboratory for Regional Pollution Control, Ministry of Education (IJRC), College of Environmental Sciences and Engineering, Peking University, Beijing 100871, China*

**Mengren Li** − *State Key Joint Laboratory of Environmental Simulation and Pollution Control, International Joint Laboratory for Regional Pollution Control, Ministry of*




https://doi.org/10.1021/acs.analchem.3c02700
Anal. Chem. 2024, 96, 1834−1842

*Education (IJRC), College of Environmental Sciences and Engineering, Peking University, Beijing 100871, China*

**Hui Wang** − *State Key Joint Laboratory of Environmental Simulation and Pollution Control, International Joint Laboratory for Regional Pollution Control, Ministry of Education (IJRC), College of Environmental Sciences and Engineering, Peking University, Beijing 100871, China*

**Shuya Hu** − *State Key Joint Laboratory of Environmental Simulation and Pollution Control, International Joint Laboratory for Regional Pollution Control, Ministry of Education (IJRC), College of Environmental Sciences and Engineering, Peking University, Beijing 100871, China;* orcid.org/0009-0002-0939-8361

**Taomou Zong** − *State Key Joint Laboratory of Environmental Simulation and Pollution Control, International Joint Laboratory for Regional Pollution Control, Ministry of Education (IJRC), College of Environmental Sciences and Engineering, Peking University, Beijing 100871, China*

**Yao Bai** − *State Key Joint Laboratory of Environmental Simulation and Pollution Control, International Joint Laboratory for Regional Pollution Control, Ministry of Education (IJRC), College of Environmental Sciences and Engineering, Peking University, Beijing 100871, China*

**Zhou Zhang** − *State Key Laboratory of Automotive Safety and Energy, Tsinghua University, Beijing 100084, China*

**Shuangde Li** − *State Key Laboratory of Multiphase Complex Systems, Institute of Process Engineering, Chinese Academy of Sciences, Beijing 100190, China*

**Shijin Shuai** − *State Key Laboratory of Automotive Safety and Energy, Tsinghua University, Beijing 100084, China*

**Yunfa Chen** − *State Key Laboratory of Multiphase Complex Systems, Institute of Process Engineering, Chinese Academy of Sciences, Beijing 100190, China*

**Song Guo** − *State Key Joint Laboratory of Environmental Simulation and Pollution Control, International Joint Laboratory for Regional Pollution Control, Ministry of Education (IJRC), College of Environmental Sciences and Engineering, Peking University, Beijing 100871, China;* orcid.org/0000-0002-9661-2313

Complete contact information is available at: https://pubs.acs.org/10.1021/acs.analchem.3c02700

### Author Contributions

N.X. conceived the study, designed the model scheme, wrote the code, collected the samples, did the experiment, processed the data, analyzed the results, and wrote the paper. X.L., K.S., Y.Q., M.L., H.W., S.H., T.Z., Y.B., and Z.Z. helped collect aerosol samples. H.X.S., Y.W., and L.Z. provided valuable suggestions. M.H., S.G., S.L., S.S., and Y.C. led the projects. All authors were participated in the results discussions and manuscript revision.

### Notes

The authors declare no competing financial interest.

## ■ ACKNOWLEDGMENTS

This study was funded by the National Key Research and Development Program of China (2022YFC3701000, task1, task4) and the National Natural Science Foundation of China (Grant Nos. 22221004, 41977179).

## ■ REFERENCES

(1) Kanakidou, M.; Seinfeld, J. H.; Pandis, S. N.; Barnes, I.; Dentener, F. J.; Facchini, M. C.; Van Dingenen, R.; Ervens, B.; Nenes, A.; Nielsen, C. J.; Swietlicki, E.; Putaud, J. P.; Balkanski, Y.; Fuzzi, S.; Horth, J.; Moortgat, G. K.; Winterhalter, R.; Myhre, C. E. L.; Tsigaridis, K.; Vignati, E.; et al. *Atmos. Chem. Phys.* **2005**, *5*, 1053−1123.

(2) Andreae, M. O.; Gelencser, A. *Atmos. Chem. Phys.* **2006**, *6*, 3131−3148.

(3) Jo, D. S.; Park, R. J.; Lee, S.; Kim, S. W.; Zhang, X. L. *Atmos. Chem. Phys.* **2016**, *16*, 3413−3432.

(4) Saleh, R. *Curr. Pollut. Rep.* **2020**, *6*, 90−104.

(5) Yan, J. P.; Wang, X. P.; Gong, P.; Wang, C. F.; Cong, Z. Y. *Sci. Total Environ.* **2018**, *634*, 1475−1485.

(6) Wang, Q. Q.; Zhou, Y. Y.; Ma, N.; Zhu, Y.; Zhao, X. C.; Zhu, S. W.; Tao, J. C.; Hong, J.; Wu, W. J.; Cheng, Y. F.; Su, H. *J. Geophys. Res.: Atmos.* **2022**, *127*, No. e2021JD035599.

(7) Zhang, A. X.; Wang, Y. H.; Zhang, Y. Z.; Weber, R. J.; Song, Y. J.; Ke, Z. M.; Zou, Y. F. *Atmos. Chem. Phys.* **2020**, *20*, 1901−1920.

(8) Feng, Y.; Ramanathan, V.; Kotamarthi, V. R. *Atmos. Chem. Phys.* **2013**, *13*, 8607−8621.

(9) Wang, X.; Heald, C. L.; Liu, J. M.; Weber, R. J.; Campuzano-Jost, P.; Jimenez, J. L.; Schwarz, J. P.; Perring, A. E. *Atmos. Chem. Phys.* **2018**, *18*, 635−653.

(10) Laskin, A.; Laskin, J.; Nizkorodov, S. A. *Chem. Rev.* **2015**, *115*, 4335−4382.

(11) Huang, R. J.; Yang, L.; Shen, J. C.; Yuan, W.; Gong, Y. Q.; Guo, J.; Cao, W. J.; Duan, J.; Ni, H. Y.; Zhu, C. S.; Dai, W. T.; Li, Y. J.; Chen, Y.; Chen, Q.; Wu, Y. F.; Zhang, R. J.; Dusek, U.; O'Dowd, C.; Hoffmann, T. *Environ. Sci. Technol.* **2020**, *54*, 7836−7847.

(12) Zeng, Y. L.; Ning, Y. L.; Shen, Z. X.; Zhang, L. M.; Zhang, T.; Lei, Y. L.; Zhang, Q.; Li, G. H.; Xu, H. M.; Ho, S. S. H. *J. Geophys. Res.: Atmos.* **2021**, *126*, No. e2021JD034906, DOI: 10.1029/2021JD034906.

(13) Wang, X. K.; Hayeck, N.; Bruggemann, M.; Abis, L.; Riva, M.; Lu, Y. Q.; Wang, B. W.; Chen, J. M.; George, C.; Wang, L. *J. Geophys. Res.: Atmos.* **2020**, *125*, No. e2020JD032706.

(14) Sun, H. L.; Biedermann, L.; Bond, T. C. *Geophys. Res. Lett.* **2007**, *34*, No. 2007GL029797.

(15) Vandeginste, B.; Essers, R.; Bosman, T.; Reijnen, J.; Kateman, G. *Anal. Chem.* **1985**, *57*, 971−985.

(16) Sanchez, E.; Kowalski, B. R. *Anal. Chem.* **1986**, *58*, 496−499.

(17) Maeder, M. *Anal. Chem.* **1987**, *59*, 527−530.

(18) Kvalheim, O. M.; Liang, Y. Z. *Anal. Chem.* **1992**, *64*, 936−946.

(19) Tauler, R.; Barcelo, D. *Trac-Trend Anal Chem.* **1993**, *12*, 319−327.

(20) Liang, Y. Z.; Kvalheim, O. M. *Anal. Chim. Acta* **1994**, *292*, 5−15.

(21) Wu, H. L.; Shibukawa, M.; Oguma, K. *J. Chemom.* **1998**, *12*, 1−26.

(22) García, I.; Sarabia, L.; Ortiz, M. C.; Aldama, J. M. *Analyst* **2004**, *129*, 766−771.

(23) Vosough, M.; Salemi, A. *Food Chem.* **2011**, *127*, 827−833.

(24) Gao, H. T.; Li, T. H.; Chen, K.; Li, W. G.; Bi, X. *Talanta* **2005**, *66*, 65−73.

(25) Debrus, B.; Lebrun, P.; Ceccato, A.; Caliaro, G.; Govaerts, B.; Olsen, B. A.; Rozet, E.; Boulanger, B.; Hubert, P. *Talanta* **2009**, *79*, 77−85.

(26) Song, K.; Guo, S.; Gong, Y. Z.; Lv, D. Q.; Wan, Z. C.; Zhang, Y.; Fu, Z. H.; Hu, K.; Lu, S. H. *Appl. Geochem.* **2023**, *151*, No. 105601.

(27) Pluskal, T.; Castillo, S.; Villar-Briones, A.; Oresic, M. *BMC Bioinf.* **2010**, *11*, No. 395.

(28) Chen, Y.; Bond, T. C. *Atmos. Chem. Phys.* **2010**, *10*, 1773−1787.

(29) Cheng, Y.; He, K. B.; Du, Z. Y.; Engling, G.; Liu, J. M.; Ma, Y. L.; Zheng, M.; Weber, R. J. *Atmos. Environ.* **2016**, *127*, 355−364.

(30) Hettiyadura, A. P. S.; Garcia, V.; Li, C. L.; West, C. P.; Tomlin, J.; He, Q. F.; Rudich, Y.; Laskin, A. *Environ. Sci. Technol.* **2021**, *55*, 2511−2521.
(31) Hettiyadura, A. P. S.; Laskin, A. *J. Mass Spectrom.* **2022**, *57*, No. e4804.
(32) Lee, D. D.; Seung, H. S. *Nature* **1999**, *401*, 788−791.
(33) Lin, P.; Fleming, L. T.; Nizkorodov, S. A.; Laskin, J.; Laskin, A. *Anal. Chem.* **2018**, *90*, 12493−12502.
(34) Lin, P.; Liu, J. M.; Shilling, J. E.; Kathmann, S. M.; Laskin, J.; Laskin, A. *Phys. Chem. Chem. Phys.* **2015**, *17*, 23312−23325.
(35) Zhou, Y.; West, C. P.; Hettiyadura, A. P. S.; Pu, W.; Shi, T. L.; Niu, X. Y.; Wen, H.; Cui, J. C.; Wang, X.; Laskin, A. *Environ. Sci. Technol.* **2022**, *56*, 4173−4186.
(36) West, C. P.; Hettiyadura, A. P. S.; Darmody, A.; Mahamuni, G.; Davis, J.; Novosselov, I.; Laskin, A. *ACS Earth Space Chem.* **2020**, *4*, 1090−1103.
(37) Siemens, K.; Morales, A.; He, Q. F.; Li, C. L.; Hettiyadura, A. P. S.; Rudich, Y.; Laskin, A. *Environ. Sci. Technol.* **2022**, *56*, 3340−3353.
(38) Lin, P.; Laskin, J.; Nizkorodov, S. A.; Laskin, A. *Environ. Sci. Technol.* **2015**, *49*, 14257−14266.
(39) Lin, P.; Bluvshtein, N.; Rudich, Y.; Nizkorodov, S. A.; Laskin, J.; Laskin, A. *Environ. Sci. Technol.* **2017**, *51*, 11561−11570.
(40) Lin, P.; Aiona, P. K.; Li, Y.; Shiraiwa, M.; Laskin, J.; Nizkorodov, S. A.; Laskin, A. *Environ. Sci. Technol.* **2016**, *50*, 11815−11824.
(41) Fleming, L. T.; Lin, P.; Roberts, J. M.; Selimovic, V.; Yokelson, R.; Laskin, J.; Laskin, A.; Nizkorodov, S. A. *Atmos. Chem. Phys.* **2020**, *20*, 1105−1129.
(42) Fleming, L. T.; Lin, P.; Laskin, A.; Laskin, J.; Weltman, R.; Edwards, R. D.; Arora, N. K.; Yadav, A.; Meinardi, S.; Blake, D. R.; Pillarisetti, A.; Smith, K. R.; Nizkorodov, S. A. *Atmos. Chem. Phys.* **2018**, *18*, 2461−2480.
(43) Bluvshtein, N.; Lin, P.; Flores, J. M.; Segev, L.; Mazar, Y.; Tas, E.; Snider, G.; Weagle, C.; Brown, S. S.; Laskin, A.; Rudich, Y. *J. Geophys. Res.: Atmos.* **2017**, *122*, 5441−5456.
(44) Xie, M. J.; Chen, X.; Hays, M. D.; Lewandowski, M.; Offenberg, J.; Kleindienst, T. E.; Holder, A. L. *Environ. Sci. Technol.* **2017**, *51*, 11607−11616.
(45) Yan, C. Q.; Zheng, M.; Desyaterik, Y.; Sullivan, A. P.; Wu, Y. S.; Collett, J. L. *J. Geophys. Res.: Atmos.* **2020**, *125*, No. e2019JD032018.
(46) Misovich, M. V.; Hettiyadura, A. P. S.; Jiang, W.; Zhang, Q.; Laskin, A. *ACS Earth Space Chem.* **2021**, *5*, 1983−1996.
(47) Yang, Z. M.; Tsona, N. T.; George, C.; Du, L. *Environ. Sci. Technol.* **2022**, *56*, 4005−4016.
(48) He, Q. F.; Li, C. L.; Siemens, K.; Morales, A. C.; Hettiyadura, A. P. S.; Laskin, A.; Rudich, Y. *Environ. Sci. Technol.* **2022**, *56*, 4816−4827.
(49) Bai, Z.; Zhang, L. Y.; Cheng, Y.; Zhang, W.; Mao, J. F.; Chen, H.; Li, L.; Wang, L. N.; Chen, J. M. *Environ. Sci. Technol.* **2020**, *54*, 14889−14898.
(50) Zeng, Y.; Shen, Z.; Takahama, S.; Zhang, L.; Zhang, T.; Lei, Y.; Zhang, Q.; Xu, H.; Ning, Y.; Huang, Y.; Cao, J.; Rudolf, H. *Geophys. Res. Lett.* **2020**, *47*, No. 2020GL087977.
(51) Jiang, H. X.; Li, J.; Sun, R.; Tian, C. G.; Tang, J.; Jiang, B.; Liao, Y. H.; Chen, C. E.; Zhang, G. *Environ. Sci. Technol.* **2021**, *55*, 10268−10279.
(52) Kuang, Y.; Shang, J.; Sheng, M. S.; Shi, X. D.; Zhu, J. L.; Qiu, X. H. *Environ. Sci. Technol.* **2023**, *57*, 909−919.


https://doi.org/10.1021/acs.analchem.3c02700
*Anal. Chem.* 2024, 96, 1834−1842